



Computational Analysis of Performance Parameters of a Gasketed Plate Heat Exchanger

Shreyas Kotian^a, Nishant Jain^b, Nachiket Methekar^c, Pranit Vartak^b

^aDepartment of Mechanical and Aerospace Engineering, University of California- San Diego, San Diego, CA, 92093, USA

^bDepartment of Mechanical Engineering, K.J. Somaiya College of Engineering, Mumbai 400077, India

^cDepartment of Industrial Engineering and Management Sciences, Northwestern University, Evanston, IL, 60208, USA

Abstract The present study aims to numerically investigate the effect of chevron angle on the thermal characteristics of a gasketed plate heat exchanger (GPHE). ANSYS FLUENT is used for numerical investigation. A computational model of the GPHE is developed using the ANSYS Design Modeler. The model was validated for flow and geometric conditions as given in Nilpueng et al. Simulations were run for $200 \leq Re \leq 1000$ on the hot side and $Re = 200$ was kept constant on the cold side. The inlet temperature of the hot fluid (water) was fixed at 70°C and the temperature of the cold fluid was fixed at 30°C. Observations were made for three different chevron angles i.e., 30°, 45°, and 60°. It was found that the heat transfer rate and the heat transfer coefficient on the hot side increase with an increase in Reynolds number. Heat transfer increases by 35.69% with an increase in chevron angle from 30° to 60°. A detailed analysis showed that the corrugations present in the GPHE are responsible for the high rates of heat transfer. Corrugations make the fluid flow turbulent even at low Reynolds numbers. This can be seen from the vorticity contours as given in **Fig. 8**. **Fig. 9** and **Fig. 10** represent the variation in heat transfer coefficient and pressure drop versus Reynolds number for different configurations respectively. Thus, results obtained from the study showed that the chevron angle plays an important role in determining the thermal characteristics of the GPHE.

Keywords Computational Analysis, Performance Parameters, Heat Exchanger

1. Introduction

Heat exchangers are the devices that provide the transfer of thermal energy between two or more fluids at different temperatures. They are mainly used in heating, cooling and heat recovery processes in industries. Gasketed plate heat exchangers have assumed importance in recent years due to its wide applications in power production, dairy plants, refrigeration and air conditioning due to its compactness, ease of cleaning and assembly/disassembly. Some of the limitations are limited operating temperature due to resistance of the gasket material and low operating pressure. Flow conditions, fluid properties and plate geometry play an important role in thermal and hydraulic performance of gasketed plate heat exchanger. The main factors affecting the performance of the heat exchanger are Reynold's number, fluid temperature, number of plates and chevron angle of the plate. Various researchers have investigated effect of these parameters through experimental and numerical studies [1-8]. Gulenoglu et al. [1] experimentally studied the thermal and hydraulic characteristics for three different plate geometries with a fixed chevron angle of 30°. It was observed that, thermal and hydraulic performance enhances with decrease in plate size. Corrugation patterns makes the fluid turbulent even at low Reynold's Number. It was seen that by increasing the port diameter and effective plate area, the pressure drop across the inlet and outlet increases. Han et al. [2] investigated heat transfer



characteristics and flow characteristics for corrugated plate geometry. The comparison between the simulation and experimental results yielded a deviation of 2°C. The pressure field indicates a decrease in fluid pressure along the flow direction. It was also found that there is a marked dead zone where the fluid flow rate is very low. Alzahran et al. [3] performed both CFD and experimental analysis on a PHE with sinusoidal corrugation. The investigation was conducted for a 60°/60° chevron angle plate covering a wide range of Reynold's Number ($500 \leq Re \leq 3000$). It was concluded that the realizable

$k - \varepsilon$ model with scalable wall function as near wall treatment provided the most accurate and consistent results. The Nusselt Number showed higher values for both higher Reynold's Number and Prandtl's Number for all simulations. Khan et al.

[4] carried out experiments on plate heat exchangers of different configurations having symmetric chevron angles. Re was varied from 500 to 2500 with water as a working fluid. It was found that Nu increases with increase in chevron angle. It was reported that Nu increases linearly with Re . At a given Re , the Nu increases four to nine times compared to flat plate at various chevron angles. Focke et al. [5] developed an experimental setup to determine the effect of corrugation inclination angle also known as chevron angle (β) on the thermohydraulic performance of plate heat exchangers. Plates with different chevron angles were tested. It was reported that increase in heat transfer and pressure drop with chevron angle reaches maximum at $\beta \approx 80^\circ$ and there after starts reducing. Dutta and Rao [6] performed experiments on 4 different PHE's with the chevron angle, β being constant at 60° and the number of plates varying. It was found out that the pressure drop, overall heat transfer coefficient increases and effectiveness decreases with increasing the Re . Durmus et al. [7] investigated the heat transfer and pressure drop in PHE with different surface profiles one with corrugations and the other with asterisk surface structure Through the experiments it was concluded that to increase the heat transfer rectangular fins are located on the pins. The efficiency of a heat exchanger increases with increasing the fluid's contact surface, pressure drop and mass flow rates due to enhanced heat transfer to the fluid. Ahn and Kim [8] estimated the heat transfer and pressure drop of the PHE for different operating conditions. Plates with chevron angle of 25° were used. Heat exchanger efficiency for the engine coolant decreased by 30% when cold water is supplied at 40°C. Corrugated plates create the separation and convergence of boundary layers. Hence even at low Re , it is capable to carry out effective heat transfer. Though various researchers have studied thermal and hydraulic performance of GPHE for different flow and geometry conditions from several years, investigation of performance of GPHE remains a topic of investigation due to turbulent flow characteristics which changes with change in flow conditions and geometry of a plate. Present study investigates effect of such a flow condition on performance of GPHE using theoretical, experimental and numerical tools.

2. Plate Geometry

The corrugated plates/chevron plates are the most important component of the gasketed plate heat exchanger. Certain number of such plates are arranged in parallel with ports for fluid entry and exit in four corners. **Fig. 1** shows geometry of the plate used in gasketed plate heat exchanger. The various geometrical parameters of the plate used in GPHE such as chevron angle, corrugation depth, corrugation pitch is illustrated in the **Fig. 1**. Geometric details of the plate used for present investigation is given in **Table 1**.



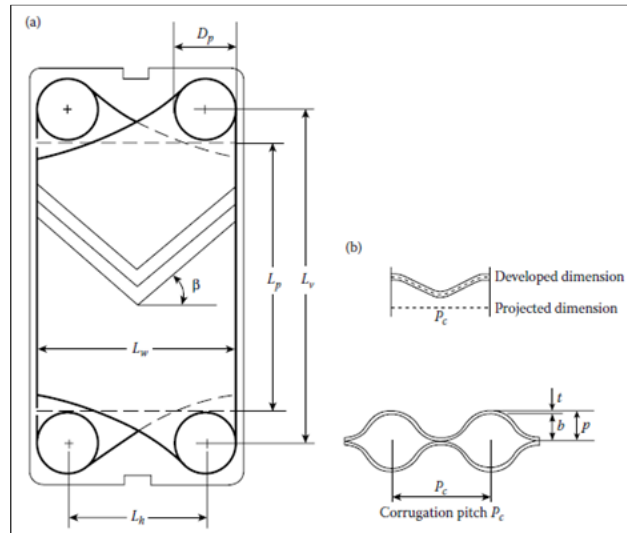


Figure 1: Main dimensions of a chevron plate; (b) developed and projected dimensions of a chevron plate cross-section normal to the direction of troughs.

Table 1: The following table describes the geometrical parameters of the GPHE under investigation.

| Geometric Parameters | Magnitude (Unit) | Description |
|------------------------------------|----------------------|---|
| Surface enlargement factor, Φ | 1.27 | Ratio between the developed area (based on corrugation pitch, P_c , and plate pitch, p) and the projected area (viz. $L_w * L_p$, where $L_w = L_h + D_p$ and $L_p = L_v - D_p$) |
| Chevron angle, β | 30°, 45°, 60° | Measure of softness (small β , low thermal High thermal hydraulic characteristics of plates. Some authors define $(\pi/2) - \beta$ as typically varies from 20° to 65° |
| Thickness of plate, t | 0.5 mm | |
| Compressed pate pack length, L_c | 8.4 mm | |
| Horizontal Port Distance, L_h | 60 mm | |
| Vertical Port Distance, L_v | 355 mm | |
| Port Diameter, D_p | 25.4 mm | |
| Corrugation Pitch, P_c | 14.2 mm | |
| Plate pitch, p | 2.8 mm | |
| Mean channel spacing, b | 2.3 mm | |
| Effective Area of Plate | 0.041 m ² | |



Methodology

Present investigation consists of theoretical, experimental and computational analysis of GPHE. Flow conditions used for the analysis are given in **Table 2**. Details about the same is explained in subsequent sections.

Table 2: Flow conditions used for the present investigation.

| Parameters | Magnitude/ Description |
|---------------------------------|------------------------|
| Working fluid (tube side) | Water |
| Working fluid (shell side) | Water |
| Inlet temperature of hot fluid | 70°C |
| Inlet temperature of cold fluid | 30°C |
| Re on cold side | 200 |
| Re on hot side | 200-1000 |

3.1 CFD Methodology

3.1.1 Mathematical Model

In present study, GPHE with three plates was modelled using ANSYS Design Modeler and meshing was done using ANSYS 2020 R1. Three different geometries with variation in chevron angles were made. The combinations used in the present study were 30°, 45° and 60°. The geometric model of GPHE with chevron angle of 60° is shown in **Fig. 2**. A trapezoidal cross section was used for the plate. Two domains were created i.e., hot and cold fluid. Inlet and outlet surfaces were defined along with adiabatic walls on the periphery of the geometry.

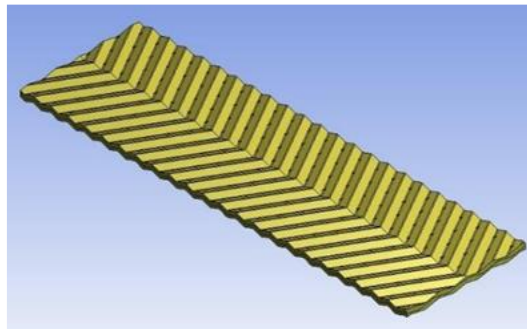


Figure 2: 3D model of GPHE geometry

3.1.2 Mesh Topology

The geometry of the system investigated (**Fig.**) was meshed using ANSYS Fluent Meshing. Element order was selected as program controlled which provides inclusion of midpoint nodes at required places and thus leading to more accuracy. The element size was selected as 0.75mm, with proximity off and curvature on. Tetrahedral element type is selected for meshing. **Fig.** shows the final mesh of the GPHE.

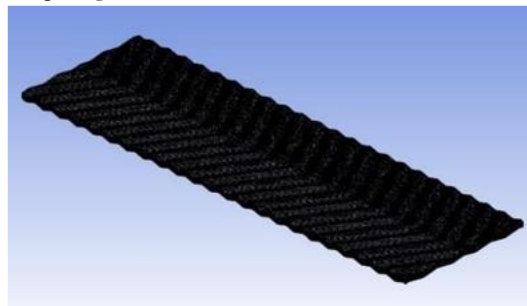


Figure 3: Final mesh of the GPHE



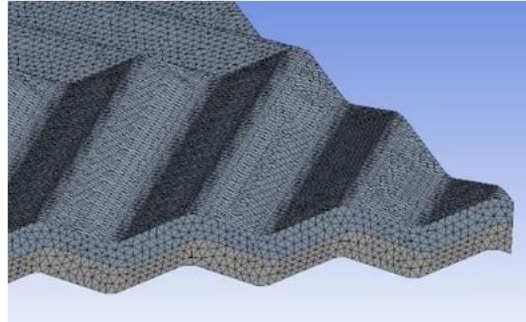


Figure 4: Close up view of the mesh.

3.1.3 Boundary Conditions

The outlets are set to pressure-outlets with a fixed value of 0 Pa, so that the inlet pressure becomes equal to the pressure drop for both the streams. The cases where the inlet temperature of the hot fluid was 70°C, and the cold fluid inlet being 30°C were investigated. The mass flow rate of the hot stream was varied from 0.00473 kg/s to 0.02365 kg/s with the mass flow rate of the cold stream being constant at 0.00935 kg/s.

3.1.4. Grid Sensitivity Analysis

The mathematical model was developed using the realizable $k-\epsilon$ turbulence model with scalable wall function. In the simulations one can notice that 0.6mm, 0.65mm, 0.7mm and 0.75mm interval size grids give very close results as seen from **Fig. 5** and **Fig. 6**. For $Re = 1000$, the deviation between 0.7mm and 0.75mm grid sizes is 0.06 % for the hot side heat transfer coefficient, and 0.04 % for the hot channel pressure drop. Based on these results, the 0.75mm mesh was finally chosen giving 4176428 nodes and 2754297 elements. Illustrations of the final mesh are shown in **Fig. 3** and **Fig. 4**.

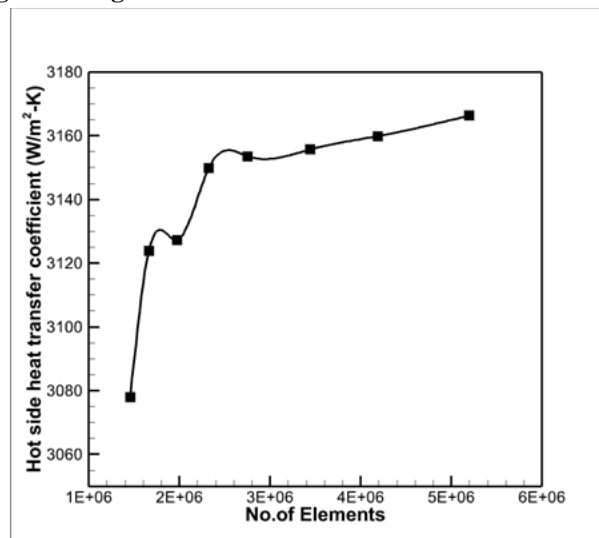


Figure 5: Hot side heat transfer coefficient in different meshes.



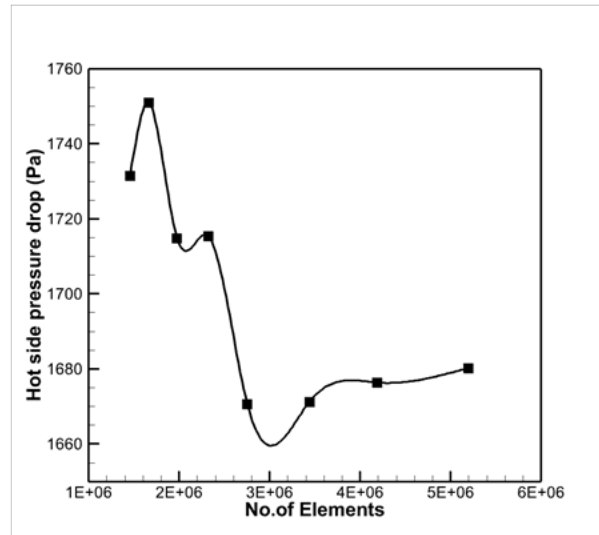


Figure 6: Hot pressure drop in different meshes.

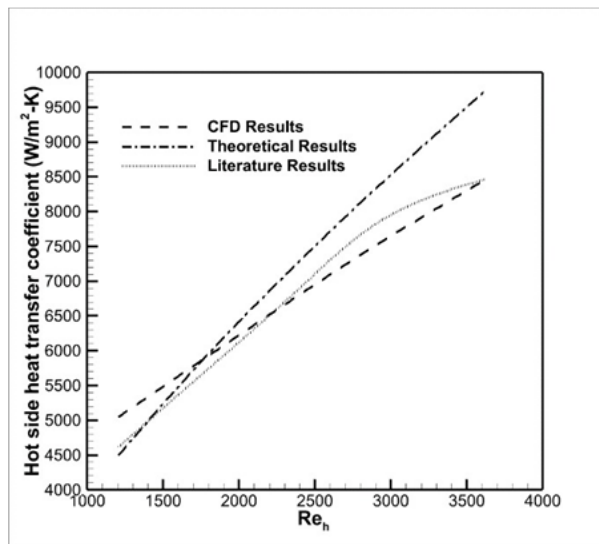


Figure 7: Hot side heat transfer coefficient vs Re for CFD, Theoretical and Literature Results.

3.1.5 Model Validation

In order to validate the computational model used in this present investigation, heat transfer coefficient for the hot fluid is estimated computationally. For model validation, flow and geometric conditions are selected as given by Nilpueng et al. [9]. The graphs obtained (Fig. 7) show very close resemblance between all the three curves with a slight deviation. This validates our computational model and methodology adopted in the present investigation for selected geometry and flow conditions.

4. Results and Discussion

Contours of vorticity magnitude are shown in Fig. 8. The inlet temperature of the hot fluid is fixed to 70°C and that of the cold fluid is fixed to 30°C. Simulations are run keeping the $Re = 200$ on the cold side with the Re on the hot side varying from 200 to 1000. The red regions indicate the corrugations and we can observe that as the chevron angle of the corrugated plate increases, the vorticity magnitude also directly increases as the corrugations become deeper. The analysis of the heat transfer coefficient contour can be done with the help of vorticity contours. As the vorticity increases, the turbulence of the fluid also increases which causes higher rates of heat transfer.



Fig. 9 shows the comparison of heat transfer coefficient for different chevron angles over a range of Reynolds number. One can observe that as the Reynolds number increases, the heat transfer coefficient is highest for the highest chevron angle at a particular value of Re . The heat transfer coefficient for the corrugated plate with a chevron angle of 60° is higher than a corrugated plate with chevron angle of 30° by about 35%. **Fig. 10** shows the comparison of pressure drop on the hot side for a corrugated plate with varying chevron angles. Simulations are run for $200 \leq Re \leq 1000$ on the hot side while the cold side Re was kept constant at 200. The pressure drop across a corrugated plate increases as the chevron angle increases. This can be validated from the fact that the contours of pressure also indicate the same. Higher the velocity, higher would be the Reynolds number and correspondingly higher pumping power and pressure drop.

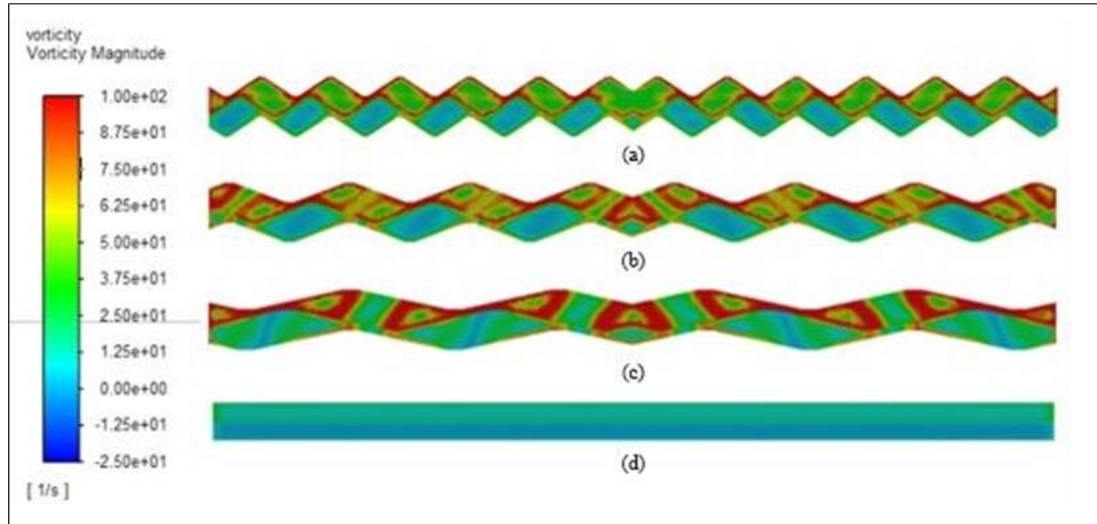


Figure 8: Vorticity contours at $Re = 1000$ for (a) chevron angle of 30° , (b) chevron angle of 45° , (c) chevron angle of 60° , (d) flat plate.

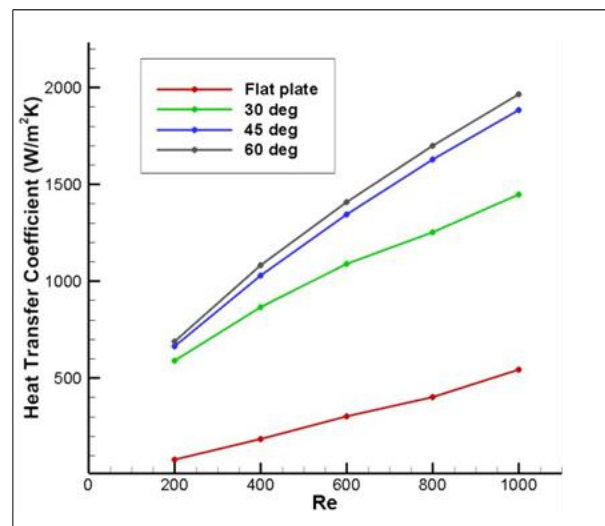


Figure 9: Heat transfer coefficient (hot side) vs Reynolds number for different plate geometries.



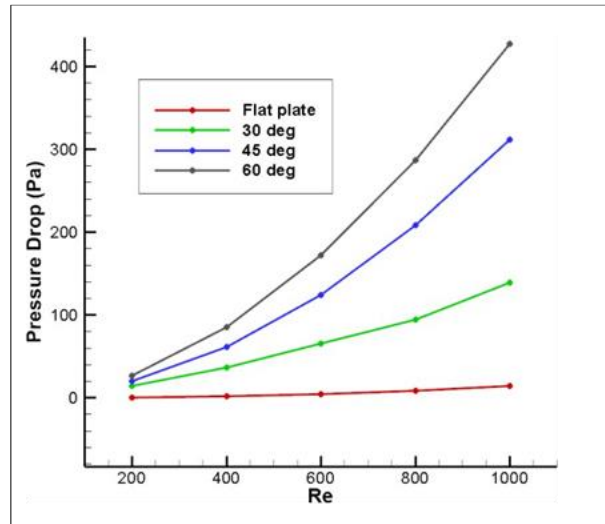


Figure 10: Pressure drop (hot side) vs Reynolds number for different plate geometries.

5. Conclusion

The present study focusses on analyzing the thermo-hydraulic performance of a gasketed plate heat exchanger. A mathematical model was developed for design and analysis of the heat exchanger at various flow conditions. The investigation is divided into three parts. The first part investigates the correlation needed to be applied to determine the thermal performance of a heat exchanger. The second part investigated the efficacy of a corrugated plate over a flat plate. The final part of the study investigated how the chevron angle affected the thermo-hydraulic performance of a gasketed plate heat exchanger. A summary of the numerical analysis drawn on the basis of the present work is given in this section. It was observed that for a particular chevron angle no single correlation is valid. There are multiple correlations available for a same chevron angle yielding different results. A corrugated plate heat exchanger is better than a flat plate having the same heat transfer area. The heat transfer in a corrugated plate was greater than the flat plate by about 262%. But there is a penalty- pressure drop. As the chevron angle was increased from 30° to 60°, the heat transfer coefficient also proportionally increased. There was an increase by 35% in the heat transfer coefficient as the chevron angle changed from 30° to 60°. However, there was a pressure drop penalty as the hot side pressure drop was about 3 times in a 60° GPHE than a 30° GPHE.

Nomenclature

| A_e | totally developed area of all thermally effective plates | Q | heat transfer rate [W] |
|-----------|--|------------|--|
| C_{max} | maximum heat capacity of fluid | R | heat capacity ratio |
| C_{min} | minimum heat capacity of fluid | Re | Reynolds number |
| C_p | heat capacity [J/kg K] | T | temperature [K or °C] |
| D_h | hydraulic diameter [m] | U | overall heat transfer coefficient [W/m ² K] |
| D_p | port diameter [mm] | b | mean channel spacing [mm] |
| L_h | horizontal port distance [mm] | f | fanning friction factor |
| L_c | compressed pate pack length [mm] | k | thermal conductivity [W/m K] |
| L_v | vertical port distance [mm] | p | plate pitch [mm] |
| L_w | width of the plate [mm] | s | entropy [J·K ⁻¹] |
| N_{cp} | number of channels per pass | t | thickness of plate [mm] |
| N_e | effective number of plates | ΔE | exergy [J] |
| N_p | number of passes | Δp | pressure drop |
| N_t | total number of plates | u, v, w | components of velocity in x, y & z directions respectively |
| P_c | corrugation Pitch [mm] | p | pressure |

| | | | |
|-------------|-------------------------------------|----------------------|--|
| Q_h | heat lost by hot fluid | t | time |
| Q_c | heat absorbed by cold fluid | $b_x, b_y,$ b_z | body forces in x, y, z Directions |
| Q_{max} | maximum heat transfer load | $k - \epsilon$ | k -epsilon model turbulence kinetic energy due to the mean velocity gradients |
| R_t | total thermal resistance | G_k | turbulence kinetic energy due to buoyancy |
| \dot{m} | mass flow rate of fluid | G_b | fluctuating dilatation constants used in the governing equations of CFD |
| \dot{m}_h | mass flow rate of cold fluid | Y_m | |
| \dot{m}_c | mass flow rate of hot fluid | $C_2, C_{1\epsilon}$ | |
| h | heat transfer coefficient | σ_k | turbulent Prandtl numbers for k |
| A | heat transfer area [m^2] | σ_ϵ | turbulent Prandtl numbers for ϵ |
| G | channel mass velocity [kg/m^2s] | S_k | user-defined source term for k |
| N | number of plates | S_ϵ | user-defined source term for ϵ |
| NTU | number of transfer units | Pr | Prandtl number |
| Nu | Nusselt number | Q | heat transfer rate [W] |
| Pr | Prandtl number | R | heat capacity ratio |

References

- [1]. C. Gulenoglu, F. Akturk, S. Aradag, N.S. Uzol, S. Kakac, Experimental comparison of performances of three different plates for gasketed plate heat exchangers, International Journal of Thermal Sciences 75 (2014) 249-
- [2]. X.H. Han, L.Q. Cui, S.J. Chen, G.M. Chen, Q. Wang, A numerical and experimental study of chevron, corrugated- plate heat exchangers, International Communications in Heat and Mass Transfer 37 (2010) 1008-1014.
- [3]. S.A. Zahrani, M.S. Islam, S.C. Saha, A thermo-hydraulic characteristics investigation in corrugated plate heat exchanger, Energy Procedia 160 (2019) 597-605.
- [4]. T.S. Khan, M.S. Khan, M.C. Chyu, Z.H. Ayub, Experimental investigation of single-phase convective heat transfer coefficient in a corrugated plate heat exchanger for multiple plate configurations, Applied Thermal Engineering 30 (2010) 1058-1065.
- [5]. W.W. Focke, J. Zachariades, I. Olivier, Effect of the corrugation inclination angle on the thermohydraulic performance of plate heat exchangers, International Journal of Heat and Mass Transfer 28 (1985) 1469-1479.
- [6]. O.Y. Dutta, B.N. Rao, Investigations on the performance of chevron type plate heat exchangers, Heat and Mass Transfer 54 (2018) 227-239.
- [7]. A. Durmus, H. Benli, I. Kurtbas, H. Gul, Investigation of heat transfer and pressure drop in plate heat exchangers having different surface profiles, International Journal of Heat and Mass Transfer 52 (2009) 1451-1457.
- [8]. J. Ahn, H.J. Kim, Heat transfer and pressure drop of a gasket-sealed plate heat exchanger depending on operating conditions across hot and cold sides, Journal of Mechanical Science and Technology 30 (5) (2016) 2325-2333.
- [9]. K. Nilpueng, T. Keawkamrop, H.S. Ahn, S. Wongwiset, Effect of chevron angle and surface roughness on thermal performance of single-phase water flow inside a plate heat exchanger, International Communications in Heat and Mass Transfer 91 (2018) 201-209.

